RESEARCH ARTICLE

Mechanism of BPh_3-Catalyzed *N*-Methylation of Amines with CO_2 and Phenylsilane: Cooperative Activation of Hydrosilane

Manussada Ratanasak,[a] Takumi Murata,[b] Taishin Adachi,[b] Jun-ya Hasegawa,*[a] and Tadashi Ema*[b]

[a] *Dr. M. Ratanasak, Prof. J. Hasegawa*
Institute for Catalysis
Hokkaido University
Kita 21, Nishi 10, Kita-ku, Sapporo, Hokkaido 001-0021 (Japan)
E-mail: hasegawa@cat.hokudai.ac.jp

[b] *T. Murata, T. Adachi, Prof. T. Ema*
Division of Applied Chemistry, Graduate School of Natural Science and Technology
Okayama University
Tsushima-naka 3-1-1, Okayama 700-8530 (Japan)
E-mail: ema@cc.okayama-u.ac.jp

Supporting information for this article is given via a link at the end of the document.

Abstract: BPh_3 catalyzes the *N*-methylation of secondary amines and the *C*-methylenation (methylene-bridge formation between aromatic rings) of *N*,*N*-dimethylanilines or 1-methylindoles in the presence of CO_2 and $PhSiH_3$, and these reactions proceed at 30–40 °C under solvent-free conditions. In contrast, $B(C_6F_5)_3$ shows little or no activity. ^{11}B NMR spectra suggested the generation of $[HBPh_3]^-$. The detailed mechanism of the BPh_3-catalyzed the *N*-methylation of *N*-methylaniline (**1**) with CO_2 and $PhSiH_3$ was studied by DFT calculations. BPh_3 promotes the conversion of two substrates (*N*-methylaniline and CO_2) into a twitterionic carbamate to give three-component species $[Ph(Me)(H)N^+CO_2^-\cdots BPh_3]$. The carbamate and BPh_3 act as the nucleophile and Lewis acid, respectively, for the activation of $PhSiH_3$ to generate $[HBPh_3]^-$, which is used to produce key CO_2-derived species, such as silyl formate and bis(silyl)acetal, essential for the *N*-methylation of **1**. DFT calculations also suggested other mechanisms involving water for the generation of $[HBPh_3]^-$ species.

Introduction

Carbon dioxide (CO_2) is a sustainable C1 source for organic synthesis, and much attention has been paid especially to the catalytic conversions of CO_2 into value-added chemicals,[1] which will be essential for the creation of carbon-neutral societies. Among various CO_2 fixation reactions, the reduction of CO_2 presents an important and interesting class of research subjects because most of the products are significant from the viewpoint of energy and chemical values.[2] Hydrosilanes are easy-to-use reductants showing moderate reactivity,[3] and the reduction of CO_2 with hydrosilanes produces silyl formates (HCO_2SiR_3), bis(silyl)acetals ($CH_2(OSiR_3)_2$), methoxysilanes (CH_3OSiR_3), or methane (Scheme 1a),[4] some of which serve as reactive intermediates. Selective formation and utilization of one of the reactive species are the key to successful reductive CO_2 fixation. For example, the catalytic reduction of CO_2 with hydrosilane in the presence of amines gives formamides, aminals, or *N*-methylamines selectively (Scheme 1b).[5–7] The chemoselectivity often depends on reaction parameters such as catalyst, hydrosilane, solvent, and temperature;[6,7] for example, amines often undergo *N*-formylation and *N*-methylation at lower and higher temperature, respectively. Because the two oxygen atoms of CO_2 are difficult to remove, various methods and catalysts for deoxygenative CO_2 conversions need to be developed.

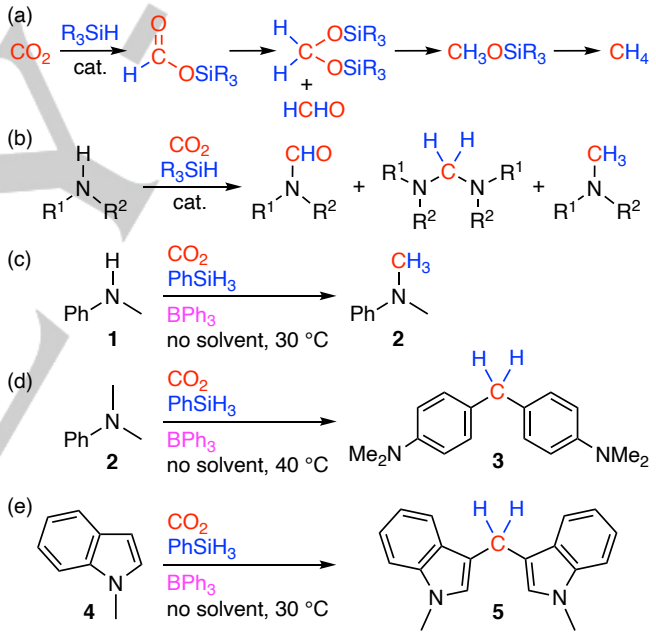

Scheme 1. (a) Reduction of CO_2 with hydrosilane. (b) *N*-Functionalization of amines. (c)–(e) Deoxygenative CO_2 conversions with BPh_3 and $PhSiH_3$.

Recently, we have reported that triphenylborane (BPh_3) smoothly catalyzed the *N*-methylation of *N*-methylaniline (**1**) with CO_2 (1 atm) and $PhSiH_3$ without solvent at 30 °C (Scheme 1c).[8] In addition, methylene-bridge formation between aromatic rings (*C*-methylenation) of *N*,*N*-dimethylaniline (**2**) or 1-methylindole (**4**) also proceeded at 30–40 °C with this catalytic system (Schemes 1d–e).[8] In sharp contrast, $B(C_6F_5)_3$ showed little or no activity under otherwise the same conditions. Although several methods for successive C–H/C–C bond formation with CO_2 have been reported,[8,9] the above deoxygenative CO_2 conversions at 30–40 °C are quite unique.[10–12] In fact, other catalysts reported so far usually require much higher temperature to achieve the *N*-methylation of amines with CO_2 and hydrosilane. Therefore, the origin of the high catalytic activity of this catalytic system composed of BPh_3 and $PhSiH_3$ is quite interesting and worthy of investigation. The elucidation of the reaction mechanism would promote the further progress of CO_2 fixation chemistry in future.

Here we report our mechanistic studies on the BPh_3-catalyzed *N*-methylation of **1** with CO_2 and $PhSiH_3$. DFT calculations revealed a cooperative mechanism for the activation of $PhSiH_3$. BPh_3 promotes the conversion of two substrates (*N*-methylaniline and CO_2) into a twitterionic carbamate to give three-component species $[Ph(Me)(H)N^+CO_2^-\cdots BPh_3]$, and the carbamate and BPh_3 act as the nucleophile and Lewis acid, respectively, for the activation of $PhSiH_3$ to generate a $[HBPh_3]^-$ species, which catalyzes the successive reduction of CO_2 to key CO_2-derived reactive species such as silyl formate, bis(silyl)acetal, and formaldehyde, which are then utilized in the *N*-methylation of **1**. Interestingly, DFT calculations also suggested hypothetical water-assisted mechanisms for the generation of $[HBPh_3]^-$ species.

Results and Discussion

BPh_3 is known to catalyze the synthesis of silyl formates from CO_2 (1 bar) and $PhSiH_3$ in CH_3CN at 40 °C,[13] while we observed no hydrosilylation of CO_2 in the absence of solvent.[8] Interestingly, the solvent-free reduction of CO_2 with BPh_3 and $PhSiH_3$ (*N*-methylation) did proceed in the presence of **1** at 30 °C to give **2** (Scheme 1c). These results suggest that **1** participates in the activation of $PhSiH_3$ and/or CO_2 under the solvent-free conditions. Based on a series of experiments,[8] we assumed two pathways from **1** to **2** (Scheme 2a). One involves the reaction of **1** with silyl formate to give *N*-methylformanilide, which is further reduced to **2**.[14] The other involves the reaction of **1** with formaldehyde or bis(silyl)acetal to give an iminium cation or its equivalent such as hemiaminal silyl ether, and the successive hydride reduction furnishes **2**. The BPh_3-catalyzed reaction of **2** with formaldehyde or its equivalent would give diarylmethane **3**. We consider $[HBPh_3]^-$ to be a key species in the catalytic cycles, for example, as shown in Scheme 2b.

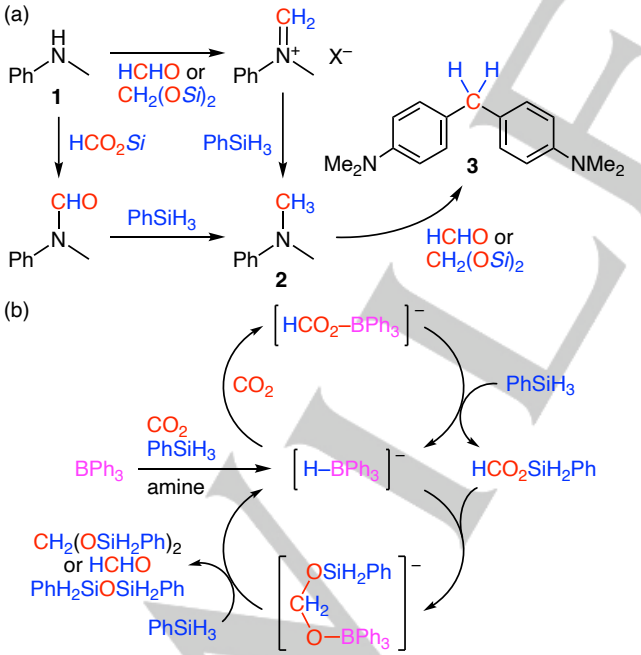

Scheme 2. (a) Plausible reaction pathways. (b) Plausible catalytic cycles.

We measured ^{11}B NMR spectra of various combinations of reactants and found specific conditions giving a signal for $[HBPh_3]^-$ species (Figures 1 and S6–S7). Figure 1c indicates that a doublet signal for a $[HBPh_3]^-$ species appeared at –7.1 ppm ($^1J_{BH}$ = 79 Hz) immediately after addition of $PhSiH_3$ (2 equiv) to a 1:1 mixture of BPh_3 and tetrabutylammonium formate, $Bu_4N^+HCO_2^-$, under N_2 (Figure 1b). The chemical shift and the coupling constant are close to the literature values for $[HBPh_3]^-$ species.[15] The intensity of this doublet signal was gradually enhanced over 20 h (Figure 1d). The fact that this is a signal for a $[HBPh_3]^-$ species was further confirmed by bubbling with CO_2; the signal was immediately changed to a broad singlet signal at 3.5 ppm (Figure 1e). We consider that the spectral changes in Figure 1 are associated with the cascade reactions starting from $[HCO_2BPh_3]^-$ (Scheme 2b); the reaction of $[HCO_2BPh_3]^-$ with $PhSiH_3$ gives $[HBPh_3]^-$ and HCO_2SiH_2Ph, and the subsequent reduction of HCO_2SiH_2Ph with $[HBPh_3]^-$ gives $[PhSiH_2OCH_2OBPh_3]^-$, which further reacts with $PhSiH_3$ to give bis(silyl)acetal or formaldehyde with the regeneration of $[HBPh_3]^-$. It is likely that $[HBPh_3]^-$ species can be accumulated under the above conditions under N_2 atmosphere. We decided to clarify the catalytic mechanism in more detail by DFT calculations.

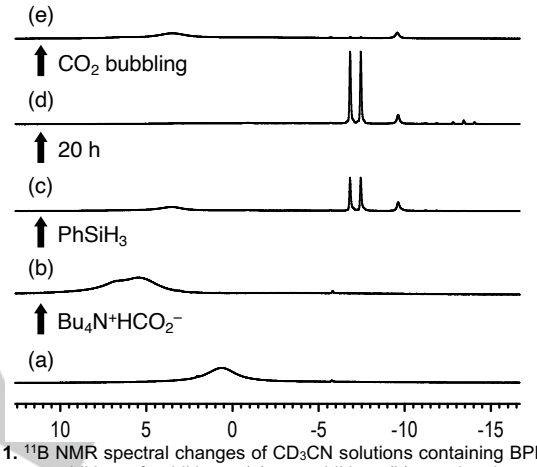

Figure 1. ^{11}B NMR spectral changes of CD_3CN solutions containing BPh_3 (0.5 mmol) upon addition of additives. (a) no additive. (b) tetrabutylammonium formate (0.5 mmol). (c) $PhSiH_3$ (1.0 mmol), after 30 min. (d) after 20 h. (e) CO_2 bubbling for 15 min. The small singlet (–9.6 ppm) and triplet (–13.4 ppm, $^1J_{BH}$ = 79 Hz) are assigned to byproducts $[Ph_3BCD_2CN]^-$ and $[H_2BPh_2]^-$, respectively.

We intensively performed DFT calculations to elucidate the mechanism for the generation of catalytically active species such as $[HBPh_3]^-$ and reactive species such as silyl formate and formaldehyde.[16] The most plausible mechanism and the potential energy profiles are shown in Figure 2, and the structures of the transition states and intermediates are given in Figure 3 and Figures S10–S20. Four chemical species (**1**, CO_2, $PhSiH_3$, and BPh_3) interact with one another to constitute complex equilibria. Among all the six two-component complexes, **1**–BPh_3 is the most stable, and BPh_3 induces the insertion of CO_2 to generate the three-component species **R**, $Ph(Me)(H)N^+CO_2^-\cdots BPh_3$ (Figure S21).[17,18] Although this ternary complex **R** is the most stable CO_2-adduct, which is driven by the binding of the oxyanion to the boron atom, **R** is less stable than binary complex **1**–BPh_3 as supported by ^{11}B NMR spectra (Figure S8). A metastable complex **I1** consisting of all the four components is also included in the equilibria. Subsequently, pentacoordinate silicate intermediate **I2** is formed from **I1** via **TS1**, where the twitterionic carbamate and BPh_3 act as the nucleophile and the Lewis acid, respectively, for the cooperative activation of $PhSiH_3$.[18] The barrierless transformation of **I2** to borohydride **I3** occurs. Importantly, **I3** is a branchpoint for catalytic cycles A and B, where silyl formate and formaldehyde are produced, respectively. In cycle A, CO_2 insertion into borohydride gives boryl formate **I5-A** via **TS2-A**.[19] The carbonyl oxygen atom of the formate moiety interacts with the silicon atom of the counter cation in **I6-A**, which is converted into pentacoordinate silicate intermediate **I7-A** via **TS3-A**. The barrierless transformation of **I7-A** to **I8-A** affords silyl formate, regenerating the resting state of the three-component catalytically active species, **R**. In cycle B, silyl formate is further reduced by borohydride **I3** via **TS2-B** to afford **I5-B** and much more stable **I6-B**. Interestingly, less stable ion pair **I5-B** has a pathway to

bis(silyl)acetal, $CH_2(OSiH_2Ph)_2$, with an activation barrier of 15.1 kcal/mol, which can be converted into formaldehyde (and siloxane) with an activation barrier of 21.5 kcal/mol (Figure S14). In contrast, more stable ion pair **I6-B** directly produces formaldehyde (and siloxane) with an activation barrier of 18.9 kcal/mol (**TS3-B**) to regenerate **R** via complexes **I7-B** and **I8-B** in equilibrium. Figure 2b clearly indicates the overall exothermic reactions with relatively low activation barriers. Both **TS1** and **TS3-B** are considered to be the rate-determining steps.

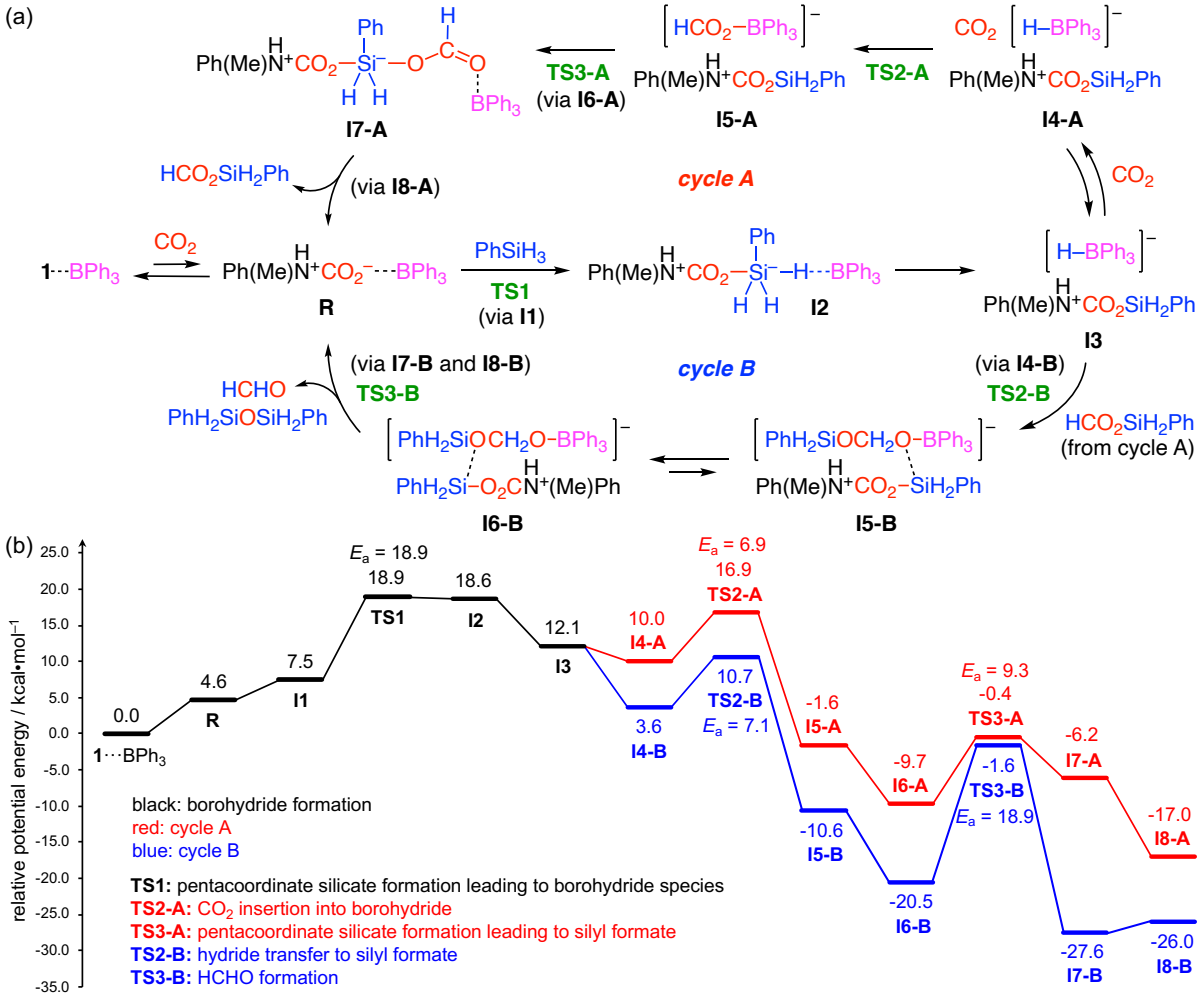

Figure 2. (a) Catalytic cycles for the generation of reactive species from CO_2 and $PhSiH_3$ with BPh_3 and **1**. (b) Potential energy profiles with E_a values in kcal/mol. DFT calculations were performed at the ωB97XD/6-31G(d) level of theory, except for the hydride of $PhSiH_3$ employing the 6-31++G(d,p) basis set. The self-consistent reaction field (SCRF) method with the polarizable continuum model (PCM) was adopted to take the solvation effect into account, and the PCM parameters for toluene were employed.

Figure 3 indicates that BPh_3, which is a moderately strong Lewis acid, promotes the borohydride formation by stabilizing the anionic species on the boron atom (Figures 3a–b), whereas BPh_3 may slow down the subsequent reactions in cycles A and B by lowering the nucleophilicity of the anionic species on the boron atom (Figures 3c–f). The Lewis acidity of the catalyst needs to be well tuned to make all the steps feasible. This hypothesis accounts for the experimental results that $B(C_6F_5)_3$ was much less active than BPh_3,[8] which is also consistent with the previous report by Okuda that $[HB(C_6F_5)_3]^-$ was much less active for CO_2 hydroboration than $[HBPh_3]^-$.[19] In the rate-determining step, **TS3-B**, the oxyanion leaves the boron atom, forming formaldehyde, and a silyloxyanion is simultaneously liberated to attack the silicon atom of the counter cation, delivering a siloxane (Figure 3f). This step would be much more disadvantageous if BPh_3 is replaced by $B(C_6F_5)_3$ because the latter binds the oxyanion much more strongly.

It is interesting to note that the borohydride species such as **I3** are likely to form H_2 by a quenching reaction with the nearby proton. Indeed, the activation barrier for this side reaction was calculated to be only 3.0 kcal/mol (Figure S15). We speculate that in reality, the proton in the counter cation of the borohydride species is hydrogen bonded with and shielded by or even deprotonated by the surrounding amines (**1** and **2**) to suppress the generation of H_2 to some degree. Under the standard reaction conditions for the *N*-methylation of **1**, we did observe the generation of a gas (bubbles), which was identified to be H_2 by GC analysis (Figure S1). Tertiary amine **2** can avoid this side reaction because the corresponding carbamate has no proton on the nitrogen atom. On the other hand, if formaldehyde is generated *in situ*, it may undergo further hydrosilylation to give methoxysilane as a byproduct. Indeed, methanol could be detected and quantified by means of GC and NMR spectroscopy after quenching with D_2O (Figures S2–S3). These byproducts, H_2 and methanol, are consistent with the catalytic mechanism (Figure 2).[20]

DFT calculations have also supported the two pathways from **1** to **2** (Scheme 2a), both of which are catalyzed by BPh_3 (Figures S9, S13, and S16–S20). One is initiated by the reaction of **1** with formaldehyde to give a hemiaminal, which is converted into an iminium cation,[21] and the subsequent borohydride reduction furnishes **2**. The other involves the reaction of **1** with silyl formate to deliver *N*-methylformanilide. Once *N*-methylformanilide is formed, **2** can be produced by using only BPh_3 and $PhSiH_3$ as confirmed previously by a control experiment.[8,14] *N*-Methylformanilide and BPh_3 act as a nucleophile and the Lewis

acid, respectively, to activate $PhSiH_3$ (Figure 4), generating an ion pair consisting of a siloxyiminium species and $[HBPh_3]^-$. Although the formation of a pentacoordinate silicate precedes the hydride transfer (Figure S16) probably because of the moderate Lewis acidity of BPh_3, for example, as compared to $B(C_6F_5)_3$, this activation mode can be classified into the Piers–Oestreich mechanism.[22–24] The subsequent reduction of the counter cation affords a hemiaminal silyl ether, which is further transformed to an iminium cation (and siloxane), and this iminium cation undergoes borohydride reduction to give **2**. Figure 4 rationalizes the remarkable functional group tolerance (selectivity) of this specific catalytic system.[8]

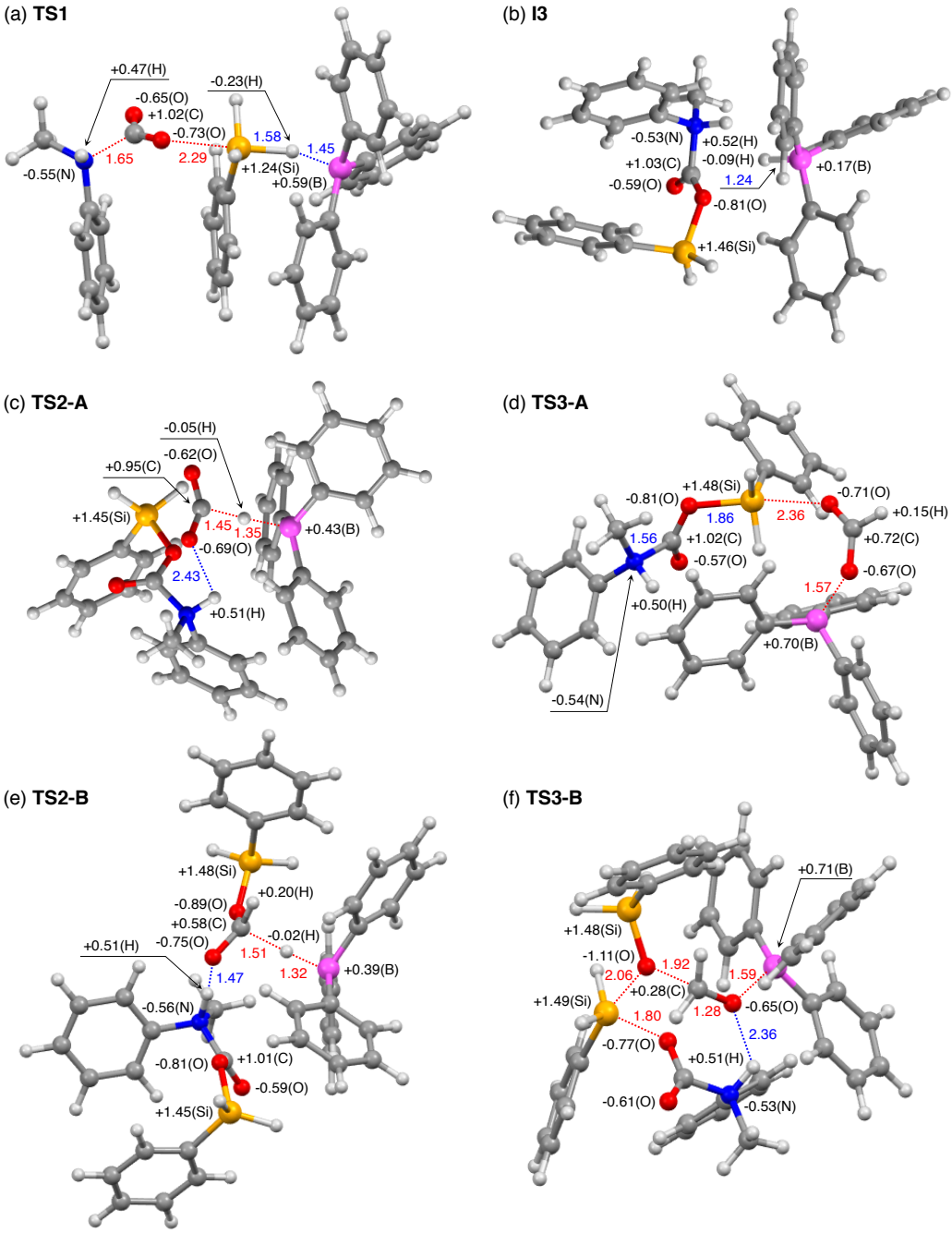

Figure 3. DFT-optimized structures of (a) **TS1**, (b) **I3**, (c) **TS2-A**, (d) **TS3-A**, (e) **TS2-B**, and (f) **TS3-B**. Distances (Å) are shown in blue or red, and NBO charges are shown in black.

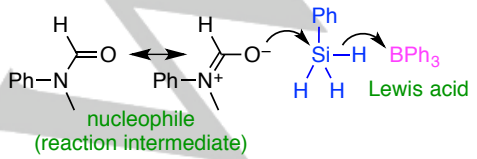

Figure 4. Cooperative activation of phenylsilane.

We explored other mechanisms for the generation of $[HBPh_3]^-$ species. We designate the activation pathway from **R** to **I3** via **I2** (Figure 2a) as type I to distinguish it from others described below. While we pursued other mechanisms by means of DFT calculations, we realized that a water molecule might act as a nucleophile to activate $PhSiH_3$ as proposed by Ingleson and co-workers for the BPh_3-catalyzed reductive amination of aldehydes with hydrosilanes in wet acetonitrile.[25] A trace amount of water may be experimentally contained in amine **1** or $PhSiH_3$. Figures 5 and S22–S25 indicate that $[HBPh_3]^-$ species can be generated relatively easily by the involvement of water. For

example, a bicarbonate ion, which is formed by the reaction of H_2O with CO_2 in the presence of **1** and BPh_3, attacks the silicon atom of $PhSiH_3$, and the hydride transfer to BPh_3 gives a $[HBPh_3]^-$ species (type II). Otherwise, a hydroxide ion, which is generated by the deprotonation of H_2O with **1**, can also activate the Si–H bond of $PhSiH_3$ to form a $[HBPh_3]^-$ species (type III). Interestingly, we have also found that if acetonitrile is used as a solvent, even in the absence of amine **1**, acetonitrile can serve as a Lewis base to weakly activate carbonic acid or water, both of which can attack the silicon atom of $PhSiH_3$ (types IV and V), whereas we have found no reasonable transition states without water even if acetonitrile is explicitly included. The pathways of types II–V, which have activation barriers that are smaller than that of type I (18.9 kcal/mol), seem to be plausible if water is present in the reaction mixture. These computational results rationalize the experimental result that the hydrosilylation of CO_2 with $PhSiH_3$ is smoothly catalyzed by BPh_3 in acetonitrile,[13] if a small amount of water is contained in the reaction mixture. Because we have previously observed no hydrosilylation of CO_2 in the absence of **1** and solvent,[8] either **1** or a weakly basic solvent like acetonitrile may be essential for the deprotonation of carbonic acid or water. The amount of water should be limited to minimize the quenching reaction of $[HBPh_3]^-$ with water, while a sufficient amount of CO_2 would favor the productive reaction of $[HBPh_3]^-$ with CO_2.

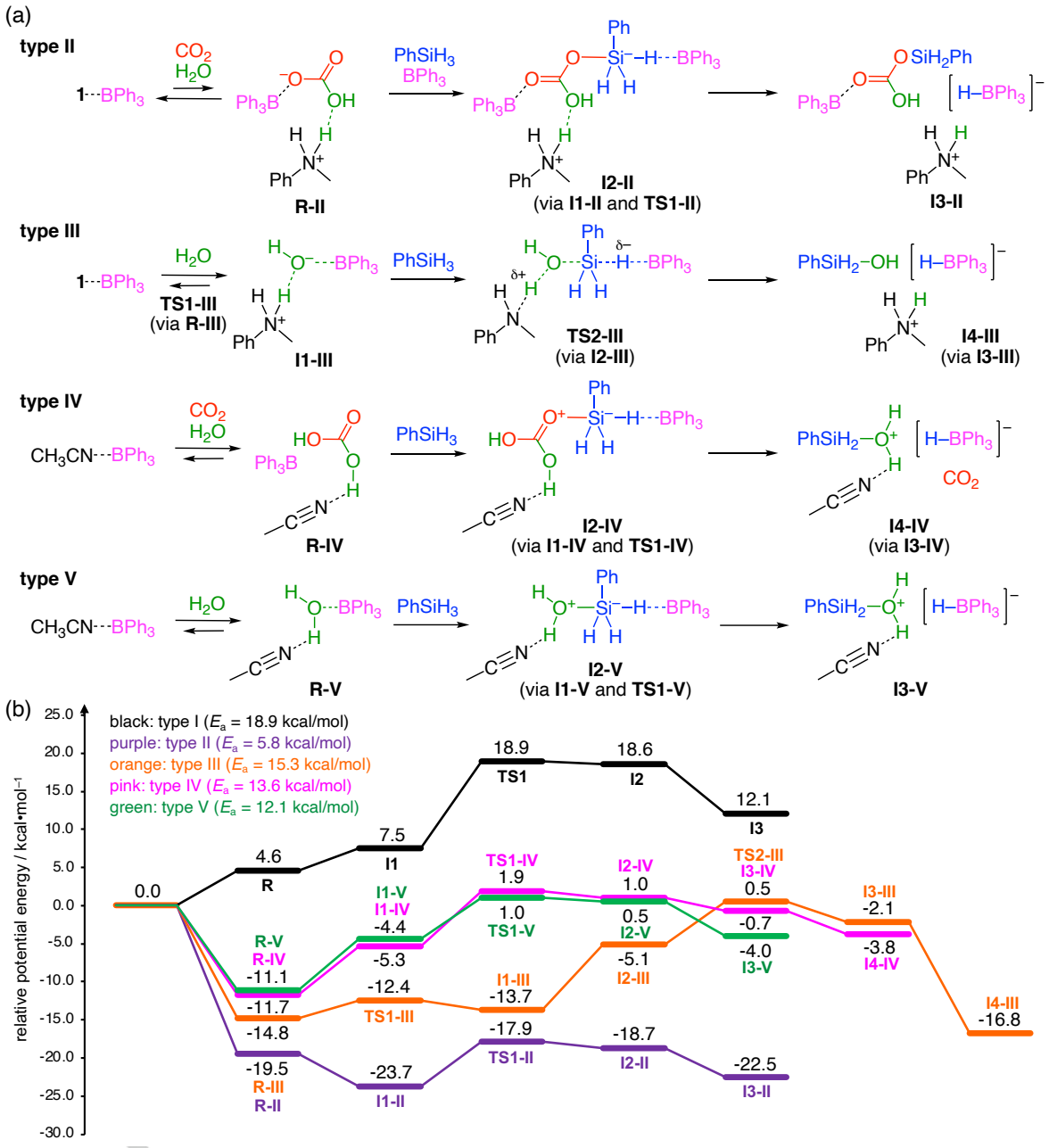

Figure 5. Comparison of the pathways to $[HBPh_3]^-$ species. (a) Hypothetical mechanisms involving a water molecule (types II–V). Formal charges are indicated on the molecular formulas, while atomic charges are shown in Figures S22–S25. (b) Potential energy profiles for types II–V, where type I is shown for comparison. DFT calculations were performed at the ωB97XD/6-31G(d) level of theory, except for the hydride of $PhSiH_3$ employing the 6-31++G(d,p) basis set. The SCRF method with the PCM was adopted to take the solvation effect into account, and the PCM parameters for toluene (types I–III) or acetonitrile (types IV and V) were employed. The energies relative to **1**–BPh_3 (types I–III) or CH_3CN–BPh_3 (types IV and V) are indicated in kcal/mol.

Conclusion

BPh_3 and $PhSiH_3$ constitute a powerful catalytic system for the deoxygenative CO_2 conversions leading to the multi-component reactions involving the C–H/C–N or C–H/C–C bond formation (Scheme 1c–e). Here we have clarified the mechanism for the deoxygenative CO_2 conversions catalyzed by BPh_3 in the presence of $PhSiH_3$ and amine **1**. DFT calculations have suggested that BPh_3 promotes the conversion of two substrates (**1** and CO_2) into a twitterionic carbamate to give three-component species **R** [$Ph(Me)(H)N^+CO_2^-\cdots BPh_3$]. The carbamate and BPh_3 act as the nucleophile and Lewis acid, respectively, for the cooperative activation of $PhSiH_3$ to generate borohydride species **I3**, which catalyzes the reduction of CO_2 to form key reactive species such as silyl formate, bis(silyl)acetal, and formaldehyde. Water may also participate in the activation of $PhSiH_3$ as a nucleophile to generate $[HBPh_3]^-$ species. The deoxygenative CO_2 fixation reactions and the reaction mechanisms that are disclosed herein will be useful for the design and development of new catalysts and reactions in future.

Acknowledgements

This work was supported by JSPS KAKENHI Grant No. 20H02780, The Yakumo Foundation for Environmental Science, and Cooperative Research Program of Institute for Catalysis, Hokkaido University (Grant 19A1003). This study was also supported by the Photoexcitonix Project at Hokkaido University and the MEXT project "Integrating Research Consortium on Chemical Science."

Keywords: Boranes • Carbon dioxide fixation • Density functional calculations • Hydrosilylation • Organocatalysis

[1] a) Q. Liu, L. Wu, R. Jackstell, M. Beller, *Nat. Commun.* **2015**, *6*, 5933; b) G. Fiorani, W. Guo, A. W. Kleij, *Green Chem.* **2015**, *17*, 1375–1389; c) B. Yu, L.-N. He, *ChemSusChem* **2015**, *8*, 52–62; d) Q.-W. Song, Z.-H. Zhou, L.-N. He, *Green Chem.* **2017**, *19*, 3707–3728; e) D. A. Sable, K. S. Vadagaonkar, A. R. Kapdi, B. M. Bhanage, *Org. Biomol. Chem.* **2021**, *19*, 5725–5757.

[2] a) A. Tlili, E. Blondiaux, X. Frogneux, T. Cantat, *Green Chem.* **2015**, *17*, 157–168; b) R. A. Pramudita, K. Motokura, *Green Chem.* **2018**, *20*, 4834–4843; c) X.-F. Liu, X.-Y. Li, C. Qiao, L.-N. He, *Synlett* **2018**, *29*, 548–555; d) X.-F. Liu, X.-Y. Li, L.-N. He, *Eur. J. Org. Chem.* **2019**, 2437–2447; e) P. Sreejyothi, S. K. Mandal, *Chem. Sci.* **2020**, *11*, 10571–10593.

[3] D. Addis, S. Das, K. Junge, M. Beller, *Angew. Chem. Int. Ed.* **2011**, *50*, 6004–6011; *Angew. Chem.* **2011**, *123*, 6128–6135.

[4] a) S. N. Riduan, Y. Zhang, J. Y. Ying, *Angew. Chem. Int. Ed.* **2009**, *48*, 3322–3325; *Angew. Chem.* **2009**, *121*, 3372–3375; b) M. Rauch, G. Parkin, *J. Am. Chem. Soc.* **2017**, *139*, 18162–18165; c) M. Rauch, Z. Strater, G. Parkin, *J. Am. Chem. Soc.* **2019**, *141*, 17754–17762; d) H. H. Cramer, B. Chatterjee, T. Weyhermüller, C. Werlé, W. Leitner, *Angew. Chem. Int. Ed.* **2020**, *59*, 15674–15681; *Angew. Chem.* **2020**, *132*, 15804–15811; e) F. Ritter, T. P. Spaniol, I. Douair, L. Maron, J. Okuda, *Angew. Chem. Int. Ed.* **2020**, *59*, 23335–23342; *Angew. Chem.* **2020**, *132*, 23535–23543.

[5] For the *N*-formylation of amines, see: a) C. Das Neves Gomes, O. Jacquet, C. Villiers, P. Thuéry, M. Ephritikhine, T. Cantat, *Angew. Chem. Int. Ed.* **2012**, *51*, 187–190; *Angew. Chem.* **2012**, *124*, 191–194; b) O. Jacquet, C. Das Neves Gomes, M. Ephritikhine, T. Cantat, *J. Am. Chem. Soc.* **2012**, *134*, 2934–2937; c) M. Hulla, F. D. Bobbink, S. Das, P. J. Dyson, *ChemCatChem* **2016**, *8*, 3338–3342; d) H. Lv, Q. Xing, C. Yue, Z. Lei, F. Li, *Chem. Commun.* **2016**, *52*, 6545–6548; e) R. Luo, X. Lin, Y. Chen, W. Zhang, X. Zhou, H. Ji, *ChemSusChem* **2017**, *10*, 1224–1232; f) M. Hulla, G. Laurenczy, P. J. Dyson, *ACS Catal.* **2018**, *8*, 10619–10630; g) M. Hulla, D. Ortiz, S. Katsyuba, D. Vasilyev, P. J. Dyson, *Chem. Eur. J.* **2019**, *25*, 11074–11079; h) Q. Zhang, X.-T. Lin, N. Fukaya, T. Fujitani, K. Sato, J.-C. Choi, *Green Chem.* **2020**, *22*, 8414–8422; i) P. Wang, Q. He, H. Zhang, Q. Sun, Y. Cheng, T. Gan, X. He, H. Ji, *Catal. Commun.* **2021**, *149*, 106195.

[6] For the *N*-methylation of amines, see: a) S. Das, F. D. Bobbink, G. Laurenczy, P. J. Dyson, *Angew. Chem. Int. Ed.* **2014**, *53*, 12876–12879; *Angew. Chem.* **2014**, *126*, 13090–13093; b) H. Niu, L. Lu, R. Shi, C.-W. Chiang, A. Lei, *Chem. Commun.* **2017**, *53*, 1148–1151; c) X. Zhang, Y. Jiang, H. Fei, *Chem. Commun.* **2019**, *55*, 11928–11931; d) K. Shinohara, H. Tsurugi, K. Mashima, *ACS Catal.* **2022**, *12*, 8220–8228.

[7] For the selective *N*-formylation/*N*-methylation of amines, see: a) C. Fang, C. Lu, M. Liu, Y. Zhu, Y. Fu, B.-L. Lin, *ACS Catal.* **2016**, *6*, 7876–7881; b) X.-F. Liu, X.-Y. Li, C. Qiao, H.-C. Fu, L.-N. He, *Angew. Chem. Int. Ed.* **2017**, *56*, 7425–7429; *Angew. Chem.* **2017**, *129*, 7533–7537; c) G. Li, J. Chen, D.-Y. Zhu, Y. Chen, J.-B. Xia, *Adv. Synth. Catal.* **2018**, *360*, 2364–2369; d) M.-Y. Wang, N. Wang, X.-F. Liu, C. Qiao, L.-N. He, *Green Chem.* **2018**, *20*, 1564–1570; e) Y. Hu, J. Song, C. Xie, H. Wu, Z. Wang, T. Jiang, L. Wu, Y. Wang, B. Han, *ACS Sustainable Chem. Eng.* **2018**, *6*, 11228–11234; f) W.-D. Li, D.-Y. Zhu, G. Li, J. Chen, J.-B. Xia, *Adv. Synth. Catal.* **2019**, *361*, 5098–5104; g) Z. Huang, X. Jiang, S. Zhou, P. Yang, C.-X. Du, Y. Li, *ChemSusChem* **2019**, *12*, 3054–3059; h) R. H. Lam, C. M. A. McQueen, I. Pernik, R. T. McBurney, A. F. Hill, B. A. Messerle, *Green Chem.* **2019**, *21*, 538–549; i) W. Zhao, X. Chi, H. Li, J. He, J. Long, Y. Xu, S. Yang, *Green Chem.* **2019**, *21*, 567–577; j) K. Takaishi, B. D. Nath, Y. Yamada, H. Kosugi, T. Ema, *Angew. Chem. Int. Ed.* **2019**, *58*, 9984–9988; *Angew. Chem.* **2019**, *131*, 10089–10093; k) D. Sarkar, C. Weetman, S. Dutta, E. Schubert, C. Jandl, D. Koley, S. Inoue, *J. Am. Chem. Soc.* **2020**, *142*, 15403–15411.

[8] T. Murata, M. Hiyoshi, S. Maekawa, Y. Saiki, M. Ratanasak, J. Hasegawa, T. Ema, *Green Chem.* **2022**, *24*, 2385–2390.

[9] For successive C–H/C–C bond formation with CO_2, see: a) X. Frogneux, E. Blondiaux, P. Thuéry, T. Cantat, *ACS Catal.* **2015**, *5*, 3983–3987; b) B. Yu, Z. Yang, Y. Zhao, L. Hao, H. Zhang, X. Gao, B. Han, Z. Liu, *Chem. Eur. J.* **2016**, *22*, 1097–1102; c) X. Ren, Z. Zheng, L. Zhang, Z. Wang, C. Xia, K. Ding, *Angew. Chem. Int. Ed.* **2017**, *56*, 310–313; *Angew. Chem.* **2017**, *129*, 316–319; d) D.-Y. Zhu, L. Fang, H. Han, Y. Wang, J.-B. Xia, *Org. Lett.* **2017**, *19*, 4259–4262; e) Z. Liu, Z. Yang, B. Yu, X. Yu, H. Zhang, Y. Zhao, P. Yang, Z. Liu, *Org. Lett.* **2018**, *20*, 5130–5134; f) X.-W. Chen, L. Zhu, Y.-Y. Gui, K. Jing, Y.-X. Jiang, Z.-Y. Bo, Y. Lan, J. Li, D.-G. Yu, *J. Am. Chem. Soc.* **2019**, *141*, 18825–18835; g) T. Murata, M. Hiyoshi, M. Ratanasak, J. Hasegawa, T. Ema, *Chem. Commun.* **2020**, *56*, 5783–5786; h) Y. Zhao, X. Liu, L. Zheng, Y. Du, X. Shi, Y. Liu, Z. Yan, J. You, Y. Jiang, *J. Org. Chem.* **2020**, *85*, 912–923; i) Y. Zhao, X. Guo, Y. Du, X. Shi, S. Yan, Y. Liu, J. You, *Org. Biomol. Chem.* **2020**, *18*, 6881–6888; j) Y. Zhao, X. Guo, X. Ding, Z. Zhou, M. Li, N. Feng, B. Gao, X. Lu, Y. Liu, J. You, *Org. Lett.* **2020**, *22*, 8326−8331; k) W.-D. Li, J. Chen, D.-Y. Zhu, J.-B. Xia, *Chin. J. Chem.* **2021**, *39*, 614–620; l) D. Zhang, C. Jarava-Barrera, S. Bontemps, *ACS Catal.* **2021**, *11*, 4568–4575.

[10] a) M. Khandelwal, R. J. Wehmschulte, *Angew. Chem. Int. Ed.* **2012**, *51*, 7323–7326; *Angew. Chem.* **2012**, *124*, 7435–7439; b) R. J. Wehmschulte, M. Saleh, D. R. Powell, *Organometallics* **2013**, *32*, 6812–6819.

[11] G. Jin, C. G. Werncke, Y. Escudié, S. Sabo-Etienne, S. Bontemps, *J. Am. Chem. Soc.* **2015**, *137*, 9563–9566.

[12] K. Takaishi, H. Kosugi, R. Nishimura, Y. Yamada, T. Ema, *Chem. Commun.* **2021**, *57*, 8083–8086.

[13] D. Mukherjee, D. F. Sauer, A. Zanardi, J. Okuda, *Chem. Eur. J.* **2016**, *22*, 7730–7733.

[14] D. Mukherjee, S. Shirase, K. Mashima, J. Okuda, *Angew. Chem. Int. Ed.* **2016**, *55*, 13326–13329; *Angew. Chem.* **2016**, *128*, 13520–13523.

[15] a) H. Osseili, D. Mukherjee, T. P. Spaniol, J. Okuda, *Chem. Eur. J.* **2017**, *23*, 14292–14298; b) F. Ritter, L. J. Morris, K. N. McCabe, T. P. Spaniol, L. Maron, J. Okuda, *Inorg. Chem.* **2021**, *60*, 15583–15592.

[16] For DFT calculations on catalytic reactions involving the hydrosilylation of CO_2, see: a) F. Huang, G. Lu, L. Zhao, H. Li, Z.-X. Wang, *J. Am. Chem. Soc.* **2010**, *132*, 12388–12396; b) Q. Zhou, Y. Li, *J. Am. Chem.*

Soc. **2015**, *137*, 10182–10189; c) J. Chen, L. Falivene, L. Caporaso, L. Cavallo, E. Y.-X. Chen, *J. Am. Chem. Soc*. **2016**, *138*, 5321–5333; d) Y. Lu, Z.-H. Gao, X.-Y. Chen, J. Guo, Z. Liu, Y. Dang, S. Ye, Z.-X. Wang, *Chem. Sci.* **2017**, *8*, 7637–7650; e) C. Zhang, Y. Lu, R. Zhao, W. Menberu, J. Guo, Z.-X. Wang, *Chem. Commun.* **2018**, *54*, 10870–10873; f) X.-Y. Li, S.-S. Zheng, X.-F. Liu, Z.-W. Yang, T.-Y. Tan, A. Yu, L.-N. He, *ACS Sustainable Chem. Eng.* **2018**, *6*, 8130–8135; g) B.-X. Leong, Y.-C. Teo, C. Condamines, M.-C. Yang, M.-D. Su, C.-W. So, *ACS Catal.* **2020**, *10*, 14824–14833.

[17] $Ph(Me)(H)N^{+}CO_2^{-}\cdots BPh_3$ (**R**) is used without deprotonation throughout the calculations because **1** is also taken as a model for **2**, which is considered to participate in the generation of reactive species for the methylene-bridge formation to give **3**. Deprotonation of **R** would enhance the nucleophilicity of the anionic oxygen atom of the carbamate.

[18] Despite many attempts, we could not detect ternary complex **R** in a mixture of **1**, BPh_3, and CO_2 by means of high-resolution mass spectrometry (ESI, positive or negative mode) and NMR or IR spectroscopy, which is probably due to the rapid dissociation of the metastable and labile complex in solutions. In fact, Figure 2b suggests that only a small amount of **R** should be generated *in situ* and that the actual activation energy in the borohydride formation step should be regarded as 18.9 kcal/mol (**TS1** relative to **1**–BPh_3).

[19] a) D. Mukherjee, H. Osseili, T. P. Spaniol, J. Okuda, *J. Am. Chem. Soc.* **2016**, *138*, 10790–10793. See also: b) Z. M. Heiden, A. P. Lathem, *Organometallics* **2015**, *34*, 1818–1827; c) R. Chambenahalli, R. M. Bhargav, K. N. McCabe, A. P. Andrews, F. Ritter, J. Okuda, L. Maron, A. Venugopal, *Chem. Eur. J.* **2021**, *27*, 7391–7401.

[20] As reported in ref. 8, a singlet signal for formaldehyde was occasionally detected at 9.73 ppm in the ^{1}H NMR spectra ($CDCl_3$) of the reaction mixtures of the *N*-methylation reaction of **1**, but only trace amounts were observed probably because formaldehyde was consumed in the *N*-methylation of **1** or the *C*-methylenation of **2** or underwent hydrosilylation with the borohydride species to give methoxysilane. Methanol was also detected in the *C*-methylenation of **2** upon hydrolysis (Figures S4–S5).

[21] R. L. Nicholls, J. A. McManus, C. M. Rayner, J. A. Morales-Serna, A. J. P. White, B. N. Nguyen, *ACS Catal.* **2018**, *8*, 3678–3687.

[22] a) D. J. Parks, W. E. Piers, *J. Am. Chem. Soc.* **1996**, *118*, 9440–9441; b) D. J. Parks, J. M. Blackwell, W. E. Piers, *J. Org. Chem.* **2000**, *65*, 3090–3098.

[23] For an S_N2-Si mechanism, see: S. Rendler, M. Oestreich, *Angew. Chem. Int. Ed.* **2008**, *47*, 5997–6000; *Angew. Chem.* **2008**, *120*, 6086–6089.

[24] Y. Hoshimoto, S. Ogoshi, *ACS Catal.* **2019**, *9*, 5439–5444.

[25] V. Fasano, M. J. Ingleson, *Chem. Eur. J.* **2017**, *23*, 2217–2224.

Entry for the Table of Contents

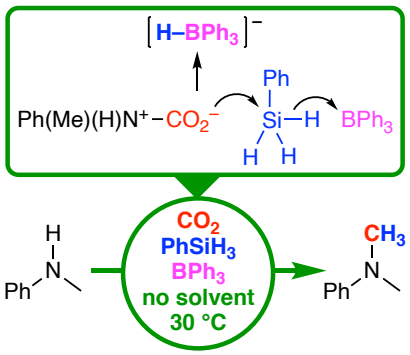

BPh_3 smoothly catalyzes the *N*-methylation of *N*-methylaniline with CO_2 and $PhSiH_3$. Twitterionic carbamate, composed of *N*-methylaniline and CO_2, and BPh_3 act as nucleophile and Lewis acid, respectively, for the activation of $PhSiH_3$ to generate $[HBPh_3]^-$, which is used to produce silyl formate and bis(silyl)acetal that are essential for *N*-methylation.